

ARTICLE

Received 3 Jun 2010 | Accepted 16 Jun 2011 | Published 12 Jul 2011

DOI:10.1038/ncomms1394

Fermi surface dichotomy of the superconducting gap and pseudogap in underdoped pnictides

Y.-M. Xu^{1,2}, P. Richard^{3,4}, K. Nakayama⁵, T. Kawahara⁵, Y. Sekiba⁵, T. Qian^{3,5}, M. Neupane¹, S. Souma⁴, T. Sato^{5,6}, T. Takahashi^{4,5}, H.-Q. Luo³, H.-H. Wen³, G.-F. Chen^{3,7}, N.-L. Wang³, Z. Wang¹, Z. Fang³, X. Dai³ & H. Ding³

High-temperature superconductivity in iron-arsenic materials (pnictides) near an anti-ferromagnetic phase raises the possibility of spin-fluctuation-mediated pairing. However, the interplay between antiferromagnetic fluctuations and superconductivity remains unclear in the underdoped regime, which is closer to the antiferromagnetic phase. Here we report that the superconducting gap of underdoped pnictides scales linearly with the transition temperature, and that a distinct pseudogap coexisting with the superconducting gap develops on underdoping. This pseudogap occurs on Fermi surface sheets connected by the antiferromagnetic wavevector, where the superconducting pairing is stronger as well, suggesting that antiferromagnetic fluctuations drive both the pseudogap and superconductivity. Interestingly, we found that the pseudogap and the spectral lineshape vary with the Fermi surface quasi-nesting conditions in a fashion that shares similarities with the nodal-antinodal dichotomous behaviour observed in underdoped copper oxide superconductors.

¹ Department of Physics, Boston College, Chestnut Hill, Massachusetts 02467, USA. ² Materials Sciences Division, Lawrence Berkeley National Laboratory, Berkeley, California 94720, USA. ³ Beijing National Laboratory for Condensed Matter Physics, and Institute of Physics, Chinese Academy of Sciences, Beijing 100190, China. ⁴ WPI Research Center, Advanced Institute for Materials Research, Tohoku University, Sendai 980-8577, Japan. ⁵ Department of Physics, Tohoku University, Sendai 980-8578, Japan. ⁶ TRiP, Japan Science and Technology Agency, Kawaguchi 332-0012, Japan. ⁷ Department of Physics, Renmin University of China, Beijing 100872, China. Correspondence and requests for materials should be addressed to H.D. (email: dingh@aphy.iphy.ac.cn).

The newly discovered iron arsenic (pnictide) superconductors^{1–4} have joined the copper oxide (cuprate) superconductors in the category of high-temperature superconductors (HTCSs). Superconductors are characterized by the size and the symmetry of the superconducting (SC) gap that forms below a critical temperature T_c . In optimally hole-doped cuprates, the SC gap function has a d -wave symmetry in momentum (k) space⁵. Its size evolves smoothly along the Fermi surface (FS) from zero at locations referred to as *nodes* to a large maximum Δ at the ‘antinodes’ that puts the value of $2\Delta/k_B T_c$ in the strong coupling regime^{6,7}. In contrast, angle-resolved photoemission spectroscopy (ARPES) studies on optimally hole-doped pnictide $\text{Ba}_{0.6}\text{K}_{0.4}\text{Fe}_2\text{As}_2$ ($T_c = 37$ K; labelled as OPD37K), have revealed isotropic gaps that have different values on different FSs^{8–11}, with strong pairing occurring on the quasi- (or nearly) nested FSs. The properties associated with the quasi-nested FSs have been described in a previous theoretical work¹².

A remarkable resemblance between these two HTCS systems is the emergence of their SC domes from an antiferromagnetic (AF) phase^{13,14} when adding extra carriers (dopants), suggesting that AF fluctuations may have a role in the SC pairing mechanism. For this reason, much attention has been devoted in the past to underdoped (UD) cuprates. In addition to the SC gap, evidence for a large doping-dependent pseudogap (PG) above T_c at the antinodes of UD cuprates has existed for some time^{15,16}. Nevertheless, debates on the interplay between superconductivity, antiferromagnetism and PG in cuprates are ongoing. Using the recently discovered pnictides, it is now possible to look into this fundamental issue from a different perspective. Unfortunately, there is no ARPES report on the UD region of hole-doped pnictides investigating the relationship between AF fluctuations and superconductivity. Thus, it is particularly important to conduct a comparison study of optimally doped (OPD) and UD pnictides to determine whether high-temperature superconductivity in cuprates and pnictides can possibly share the same mechanism.

Here we focus mainly on underdoped $\text{Ba}_{0.75}\text{K}_{0.25}\text{Fe}_2\text{As}_2$ ($T_c = 26$ K; labelled as UD26K). We observe that the SC gaps scale with T_c in the UD regime, suggesting that the gap size is controlled by the pairing strength. In addition, we reveal the existence of a 18 meV pseudogap on a quasi-nested FS pocket that coexists in momentum with the SC gap at low temperature but survives up to $T^* = 115 - 125$ K, temperature at which it completely fills in. Its band-selectivity strongly suggests an origin related to AF fluctuations. Moreover, the evolution of the spectral lineshape on underdoping indicates a dichotomy behaviour between unnested and quasi-nested FSs that shows striking similarities with the nodal–antinodal dichotomy found in cuprates, and that is naturally explained in pnictides in terms of short-range AF scattering.

Results

Superconducting gaps in underdoped pnictides. As illustrated in Figure 1d, the FS of UD26K differs from that of the OPD material previously reported^{8,9,11,17} only by the size of the holelike and electronlike FS pockets, which become, respectively, smaller and larger in UD26K and satisfy the Luttinger theorem (Supplementary Discussions for the electron counting). Similarly to the OPD sample, the quasi-nesting condition between the inner hole-FS (α) and the electron-FSs is maintained, albeit slightly weakened in the UD samples. We performed high-resolution measurements on all the FS pockets observed. Below T_c , we observe the opening of SC gaps at their corresponding Fermi vectors (k_F). As with the OPD compound^{8,9,11}, these gaps are isotropic within experimental uncertainties (Supplementary Discussion for the superconducting gap symmetry). To characterize these SC gaps further, temperature (T)-dependent ARPES measurements have been performed on different FS sheets (α , β and γ,δ). We show in Figure 1a–c spectra at various k_F positions, which have been symmetrized to remove

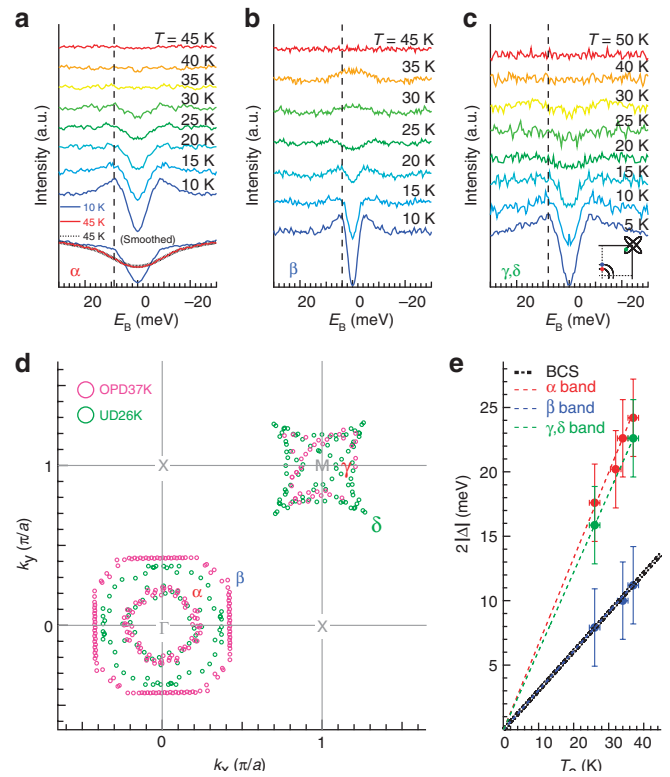


Figure 1 | SC gaps and FS of UD pnictides. (a–c) show the T dependence of the symmetrized energy distribution curves (EDCs) of $\text{Ba}_{0.75}\text{K}_{0.25}\text{Fe}_2\text{As}_2$ ($T_c = 26$ K) divided by a smoothed spectrum recorded above T_c (45–50 K) on the α , β and γ,δ FSs, respectively. The corresponding momentum locations are given in the inset of (c) (red, blue and green dots for the α , β and γ,δ FSs, respectively). Dashed lines indicate the QP peak position at low T , which can be regarded as the SC gap value. We find $\Delta_\alpha(0) = 8.5$ meV, $\Delta_\beta(0) = 4.0$ meV and $\Delta_{\gamma,\delta}(0) = 7.8$ meV. The raw curves obtained at 10 K (blue) and 45 K (red) for the α FS, as well as the smoothed 45 K (black dashed), are shown at the bottom of panel (a) as examples. (d) Comparison of FS contours between the OPD37K and UD26K samples. The dots indicate Fermi wave vectors extracted from ARPES measurements above T_c by tracing the peak position of momentum distribution curves (MDCs). (e) Full SC gap values (2Δ) versus T_c . The dashed red, blue and green lines are linear fits of the SC gaps on the α , β and γ,δ FSs passing through the origin. The dashed black line is the BCS line with a slope of $3.52 k_B$. We defined the vertical error bars as twice the derivation that we get by fitting the SC coherent peaks with Lorentzian functions. The horizontal error bars represent the transition width measured by transport experiments.

the effect of the Fermi function and then normalized by the corresponding normal state spectra. We clearly observe the opening of SC gaps on all the FS sheets at low T and their disappearance above T_c . The SC gap value (Δ) on each FS sheet of the UD26K samples is reduced by approximately 30% as compared with the OPD37K samples^{8,11}, which is almost the same as the reduction of the transition temperature (from 37 to 26 K). Interestingly, the 2Δ values vary linearly with T_c from moderate underdoping to optimal doping, as illustrated in Figure 1e. Thus, T_c is determined by the energy scale of the pairing gap within this range. The FS-dependent but doping-independent $2\Delta/k_B T_c$ ratio varies from typical BCS values (for the β FS) to strong coupling values on the quasi-nested FS sheets. A good agreement between the T_c (doping) dependence of H_{c2} deduced from ARPES and transport measurements supports the bulk nature of the linear scaling of Δ and T_c (Supplementary Figure S2). It reinforces the notion that T_c in UD pnictides is

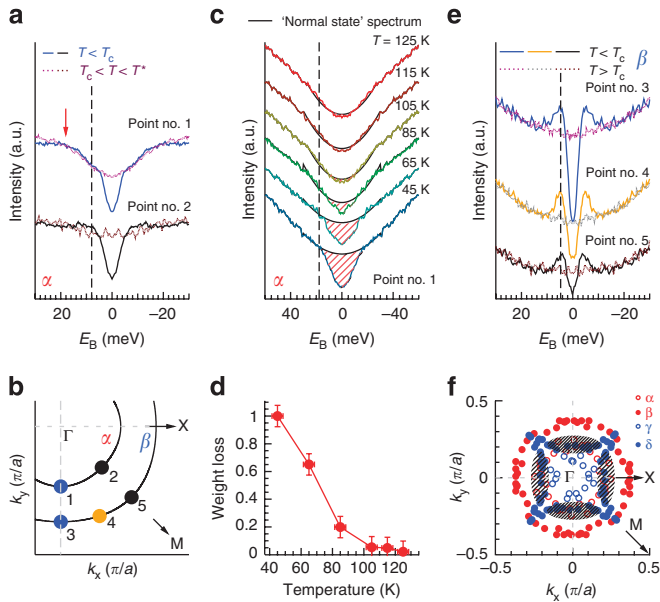


Figure 2 | Momentum dependence of the PG in $\text{Ba}_{0.75}\text{K}_{0.25}\text{Fe}_2\text{As}_2$ ($T_c = 26\text{ K}$). (a) Symmetrized EDCs of UD26K pnictide measured below and above T_c at two different locations on the α FS (points no. 1 and no. 2 in panel (b)). The red arrow indicates that the PG is -18 meV , and the dashed vertical line shows that the SC gap on the α FS is -8 meV . (b) Schematic FS plot near the Γ point indicating the measurement locations of spectra presented in (a, c and e). (c) T dependence of the symmetrized EDCs of UD26K measured at point no. 1 on the α FS above T_c . The vertical dashed line indicates the energy scale of the PG (18 meV). The shaded regions represent the spectral weight loss in the PG state. It is obtained by subtracting the symmetrized EDCs from a quadratic background. (d) T dependence of the relative weight loss (normalized by the one obtained at $T = 45\text{ K}$) in the PG state of UD26K. The error bars represent the uncertainty in calculating the relative weight loss. (e) Similar as (a) but for the β FS (points no. 3, no. 4 and no. 5). The dashed line shows the SC gap on the β FS (4 meV). (f) Electronlike FS contours of UD26K shifted to the Γ point by the (π, π) wave vector to illustrate the quasi-nesting conditions. The regions where the electronlike and holelike FSs ‘overlap’ are highlighted by shadowed areas.

controlled by the pairing strength, which is apparently different from the trend observed in some studies of cuprates where the SC gap anti-correlates with T_c on underdoping. Our results on UD pnictides are more in-line with a recent report suggesting that the SC gap in UD cuprates at the tip of the nodal ‘arc’ region scales with T_c (ref. 18) and may reflect the ‘true’ SC gap magnitude.

Pseudogap and interband scattering in underdoped pnictides.

When looking at the raw spectra recorded above T_c along the α FS of UD26K as shown in Figure 2a, we observe an additional feature around 18 meV with a clear k dependence: whereas a significant decrease of spectral weight below 18 meV is quite obvious in the spectrum recorded along the Γ -X direction (point no. 1), the spectral weight loss below 18 meV becomes negligible along the Γ -M direction (point no. 2). Unlike the SC gap, that feature survives in the normal state and hereafter we refer to it as a pseudogap. The temperature-dependence of the PG at point no. 1, given in Figure 2c, is similar to that of UD cuprates: it gradually fills up as temperature increases and eventually closes around $T^* = 115\text{--}125\text{ K}$, a temperature much higher than T_c . This observation can be expressed in a more quantitative method using the temperature evolution of the spectral weight loss below 18 meV , which is displayed in Figure 2d. Because, below T_c it coexists with the SC gap at a different energy

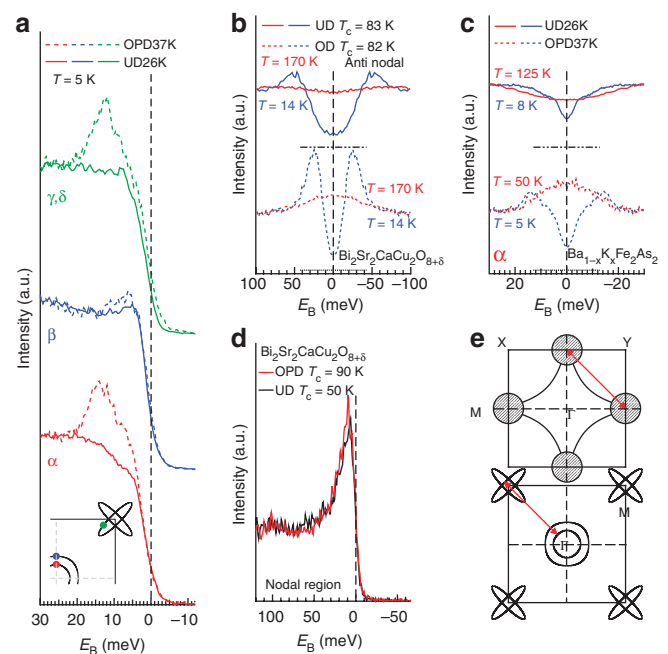


Figure 3 | Comparison of the dichotomous behaviour in the spectral lineshape of UD cuprates and UD pnictides. (a) Comparison between the EDCs of OPD37K (dashed line) and UD26K (solid line) samples below T_c on different FS sheets (red, green, and blue dots in the inset). (b) Comparison of the symmetrized EDCs at the antinodal k_f point of an overdoped (OD) Bi2212 sample ($T_c = 82\text{ K}$; dashed lines) and an UD Bi2212 sample ($T_c = 83\text{ K}$; solid lines), measured below (blue) and above (red) T_c . The black dashed (dotted) line indicates the zero intensity position of the OD Bi2212 (UD Bi2212) sample. (c) Comparison between the symmetrized EDCs of OPD37K (dashed) and UD26K (solid) at the k_f point of the α FS along Γ -M. Blue and red curves refer to spectra measured below and above T_c , respectively. (d) Comparison between the EDCs of the OPD (red) and UD (black) $\text{Bi}_2\text{Sr}_2\text{CaCu}_2\text{O}_{8+\delta}$ (Bi2212) samples measured at 10 K at the nodal point. (e) Schematic diagrams illustrating that the AF (π, π) wave vector connects the antinodal regions in hole-doped cuprates, and the inner holelike FS and the electronlike FSs in hole-doped pnictides.

scale, the PG is likely to have an origin that differs from the pairing gap. In fact, the effect of this PG below T_c can be mostly removed by dividing out a spectral function recorded slightly above T_c (45 K), revealing a more pronounced SC coherence peak, as indicated in Figure 1a. However, it is important to stress that unlike the conventional gap-opening phenomenon, there is no long-range magnetic order observed in the UD $\text{Ba}_{0.75}\text{K}_{0.25}\text{Fe}_2\text{As}_2$ samples above the SC transition^{19–21}. Therefore, the observed PG does not appear to be associated with a phase transition at T^* , which is most likely a crossover temperature scale. It is also worth noting that the coexistence of the PG and the SC gap in the same pnictide spectra is similar to recent observation of the coexistence of PG and SC gap at the antinodes of UD cuprates²².

To understand the origin of the PG, we recorded spectra along the β FS as well. In contrast to our observation for the α FS, the spectra along the β FS are almost identical, with no sign of PG (Fig. 2e). A natural way to explain the k dependence of the PG is to invoke (π, π) interband scattering. Indeed, NMR experiments have provided evidence that AF spin fluctuations appear when the holelike FS emerges at the Γ point in electron-doped pnictides, thus associating the AF fluctuations with (π, π) interband scattering^{23,24}. As shown in Figure 2f, where the electronlike FS contours centred at the M point are shifted by the (π, π) wave vector to ‘overlap’ with the holelike FS contours centred at Γ , the β FS does not significantly overlap with

the electronlike FSs. In contrast, we expect much stronger scattering between the α band and the M -centred electronlike bands, especially along the Γ - X direction. This is consistent with our observation of a well-developed 18 meV energy scale along the Γ - X direction for the α band of UD26K.

If (π, π) interband scattering is strong enough to induce a PG in UD pnictides, one expects the quasiparticle (QP) spectral weight to exhibit a similar FS dependence. In Figure 3a, we compare the spectra of UD26K and OPD37K for different FSs. Whereas the QP spectral weight for the β FS remains relatively constant with underdoping, a significant QP weight suppression occurs on the α and the electronlike FS sheets, which are quasi-nested by the (π, π) wave vector. We can thus summarize our findings on UD pnictides by distinguishing two different behaviours on two types of FS sheets: (i) quasi-nested FSs are accompanied by large SC gaps, the formation of a PG, and a strong QP spectral weight suppression on underdoping; (ii) FSs that are not quasi-nested are accompanied by a smaller SC gap, the absence of PG, and a quite robust QP on underdoping.

Discussion

Even though there exists no direct proof linking the origin of the PG and the pairing mechanism in the cuprates and in the pnictides, it is instructive at this stage to compare the two families of HTCSs. It is well known that UD cuprates also exhibit a k dependent QP weight suppression. Whereas the nodal QP remains robust, the antinodal QP loses integrity quickly with underdoping. This nodal-antinodal dichotomy²⁵ is illustrated in Figure 3b,d for the cuprate superconductor $\text{Bi}_2\text{Sr}_2\text{CaCu}_2\text{O}_{8+\delta}$. In the antinodal region of hole UD cuprates, the QPs can be scattered strongly by spin fluctuations via the (π, π) AF wave vector. Similarly, the SC phase of the pnictides emerges when doping away from the AF spin-density-wave phase in the parent compounds, and AF fluctuations exist in the UD region^{19,24,26}. Such an AF-fluctuations scenario is consistent with the observed FS-dependent QP suppression. On sections of FS that are approximately connected by the AF wave vector, the similarities in the spectral lineshape of pnictides and cuprates are striking. In the overdoped and OPD regions, both materials show a well-defined Bogoliubov quasiparticle peak in the SC state and a broadened single peak above T_c , as shown in Figure 3b,c. On underdoping, the SC Bogoliubov quasiparticle weight of both materials is rapidly weakened, and the near E_F spectral function above T_c switches from a peak to a dip.

The origin of the PG is clearly an important part of the physics of both families of HTCSs. In the pnictides, it is quite natural to attribute its origin to AF fluctuations, because it emerges near an AF phase, and its properties are shaped by the AF wave vector. Our observations of the SC coherence suppression and the reduction of the SC gap on underdoping, as well as the emergence of a PG that coexists with the SC gap below T_c , support the scenario where the PG is the offspring of a competing state, although the SC pairing itself may be mediated by AF fluctuations, as suggested by various experiments^{8,24,26,27} and theoretical works^{12,28–31}. In particular, a functional renormalization group approach has been applied to both cuprates and pnictides, suggesting that the pairing in both materials could be driven by AF correlations and enhanced by (π, π) FS quasi-nesting³². We caution that whereas AF correlations increase in pnictides on underdoping from the optimal concentration²⁴, the FS quasi-nesting conditions degrade slowly. This possibly implies that long-range spin-density-wave in the pnictides is not driven solely by FS nesting, as previously suggested theoretically³³. Nevertheless, the stronger SC pairing ($2\Delta/k_B T_c \sim 7$) and the PG observed in the quasi-nested FS sheets connected by the AF wave vector support the AF origin of both the SC gap and the PG in the pnictides. The observation of similar dichotomous behaviours in UD pnictides and UD cuprates raises the possibility for a unifying picture of HTCSs involving AF fluctuations and calls for

further experimental and theoretical works beyond the scope of the present study.

Methods

Sample preparation. The high quality single crystals of $\text{Ba}_{0.75}\text{K}_{0.25}\text{Fe}_2\text{As}_2$ used in our study were grown by the self-flux method. The T_c of the sample has been estimated to be $T_c^{\text{mid}} = 26$ K from magnetic susceptibility measurements, with a transition width of about 3 K (Supplementary Fig. S1). The nominal composition is consistent to the K-content determined by energy-dispersive X-ray spectroscopy. Low-energy electron diffraction on a measured surface shows a sharp 1×1 patterns indicating that the sample surface has a fourfold symmetry without any detectable surface reconstruction down to 80 K.

ARPES experiments. High-resolution ARPES measurements were performed in the photoemission laboratory of Tohoku University using a high-flux microwave-driven Helium source (He I α resonance line, $h\nu = 21.218$ eV) with an energy resolution of 3 meV, and a momentum resolution of 0.007 \AA^{-1} . We used a VG-SCIENIA ESE2002 spectrometer as detector. Samples were cleaved *in situ* at 10 K and measured at 5–50 K in a working vacuum better than 5×10^{-11} Torr (for the PG measurements, the temperature was increased up to 125 K and the vacuum remained better than 1×10^{-10} Torr at 125 K). Some experiments were also performed at the Wadsworth beamline of Synchrotron Radiation Center with an energy resolution of 10 meV and a momentum resolution of 0.02 \AA^{-1} . A VG-SCIENIA R4000 analyser was used for synchrotron measurements. The mirror-like sample surfaces were found to be stable without obvious degradation during measurement periods of 3 days (30 h for synchrotron measurements). The Fermi level of the samples was referenced to that of a gold film evaporated onto the sample holder. We observed that the SC gap closes around the bulk T_c (Fig. 1), which suggests that the present ARPES results reflect the bulk properties. We have confirmed the reproducibility of the ARPES data on more than ten sample surfaces and through thermal cycles across T_c .

References

- Kamihara, Y. *et al.* Iron-based layered superconductor $\text{La}[\text{O}_{1-x}\text{F}_x]\text{FeAs}$ ($x=0.05-0.12$) with $T_c=26$ K. *J. Am. Chem. Soc.* **130**, 3296–3297 (2008).
- Chen, X. H., Wu, T., Wu, G., Liu, R. H., Chen, H. & Fang, D. F. Superconductivity at 43 K in samarium-arsenide oxides $\text{SmFeAsO}_{1-x}\text{F}_x$. *Nature* **453**, 761–762 (2008).
- Chen, G. F. *et al.* Superconductivity at 41 K and its competition with spin-density-wave instability in layered $\text{CeO}_{1-x}\text{F}_x\text{FeAs}$. *Phys. Rev. Lett.* **100**, 247002 (2008).
- Ren, Z. A. *et al.* Superconductivity at 55 K in iron-based F-doped layered quaternary compound $\text{Sm}[\text{O}_{1-x}\text{F}_x]\text{FeAs}$. *Chin. Phys. Lett.* **25**, 2215 (2008).
- Tsuei, C. C. & Kirtley, J. R. Pairing symmetry in cuprate superconductors. *Rev. Mod. Phys.* **72**, 696 (2000).
- Shen, Z.-X. *et al.* Anomalously large gap anisotropy in the a - b plane of $\text{Bi}_2\text{Sr}_2\text{CaCu}_2\text{O}_{8+\delta}$. *Phys. Rev. Lett.* **70**, 1553 (1993).
- Ding, H. *et al.* Angle-resolved photoemission spectroscopy study of the superconducting gap anisotropy in $\text{Bi}_2\text{Sr}_2\text{CaCu}_2\text{O}_{8+x}$. *Phys. Rev. B* **54**, R9678 (1996).
- Ding, H. *et al.* Observation of Fermi-surface-dependent nodeless superconducting gaps in $\text{Ba}_{0.6}\text{K}_{0.4}\text{Fe}_2\text{As}_2$. *Europhys. Lett.* **83**, 47001 (2008).
- Zhao, L. *et al.* Multiple nodeless superconducting gaps in $(\text{Ba}_{0.6}\text{K}_{0.4})\text{Fe}_2\text{As}_2$ superconductor from angle-resolved photoemission spectroscopy. *Chin. Phys. Lett.* **25**, 4402–4405 (2008).
- Kondo, T. *et al.* Momentum dependence of the superconducting gap in $\text{NdFeAsO}_{1-x}\text{F}_x$ single crystals measured by angle resolved photoemission spectroscopy. *Phys. Rev. Lett.* **101**, 147003 (2008).
- Nakayama, K. *et al.* Superconducting gap symmetry of $\text{Ba}_{0.6}\text{K}_{0.4}\text{Fe}_2\text{As}_2$ studied by angle-resolved photoemission spectroscopy. *Europhys. Lett.* **85**, 67002 (2009).
- Cvetkovic, V. & Tesanovic, Z. Multiband magnetism and superconductivity in Fe-based compound. *Europhys. Lett.* **85**, 37002 (2009).
- Cruz, C. D. L. *et al.* Magnetic order close to superconductivity in the iron-based layered $\text{LaO}_{1-x}\text{F}_x\text{FeAs}$ systems. *Nature* **453**, 899–902 (2008).
- Dong, J. *et al.* Competing orders and spin-density-wave instability in $\text{La}(\text{O}_{1-x}\text{F}_x)\text{FeAs}$. *Europhys. Lett.* **83**, 27006 (2008).
- Ding, H. *et al.* Spectroscopic evidence for a pseudogap in the normal state of underdoped high T_c superconductor. *Nature* **382**, 51–54 (1996).
- Loeser, A. G. *et al.* Excitation gap in the normal state of underdoped $\text{Bi}_2\text{Sr}_2\text{CaCu}_2\text{O}_{8+\delta}$. *Science* **273**, 325–329 (1996).
- Ding, H. *et al.* Electronic structure of optimally doped pnictide $\text{Ba}_{0.6}\text{K}_{0.4}\text{Fe}_2\text{As}_2$: a comprehensive angle-resolved photoemission spectroscopy investigation. *J. Phys. Condens. Matter* **23**, 135701 (2011).
- Hufner, S., Hossain, M. A., Damascelli, A. & Sawatzky, G. A. Two gaps make a high-temperature superconductor? *Rep. Prog. Phys.* **71**, 062501 (2008).

19. Matano, K. *et al.* Anisotropic spin fluctuations and multiple superconducting gaps in hole-doped $\text{Ba}_{0.7}\text{K}_{0.3}\text{Fe}_2\text{As}_2$: NMR in a single crystal. *Europhys. Lett.* **87**, 27012 (2009).
20. Rotter, M., Pangerl, M., Tegel, M. & Johrendt, D. Superconductivity and crystal structures of $(\text{Ba}_{1-x}\text{K}_x)\text{Fe}_2\text{As}_2$ ($x=0-1$). *Angew. Chem. Int. Ed.* **47**, 7947 (2008).
21. Urbano, R. R. *et al.* Distinct high- T transitions in underdoped $\text{Ba}_{1-x}\text{K}_x\text{Fe}_2\text{As}_2$. *Phys. Rev. Lett.* **105**, 107001 (2010).
22. Ma, J. *et al.* Coexistence of competing orders with two energy gaps in real and momentum space in the high temperature superconductor $\text{Bi}_2\text{Sr}_{2-x}\text{La}\text{CuO}_{6+\delta}$. *Phys. Rev. Lett.* **101**, 207002 (2008).
23. Sekiba, Y. *et al.* Electronic structure of heavily electron-doped $\text{BaFe}_{1.7}\text{Co}_{0.3}\text{As}_2$ studied by angle-resolved photoemission. *New J. Phys.* **11**, 025020 (2009).
24. Ning, F. L. *et al.* Contrasting spin dynamics between underdoped and overdoped $\text{Ba}(\text{Fe}_{1-x}\text{Co}_x)_2\text{As}_2$. *Phys. Rev. Lett.* **104**, 037001 (2010).
25. Zhou, X. J. *et al.* Dichotomy between nodal and antinodal quasiparticles in underdoped $\text{La}_{2-x}\text{Sr}_x\text{CuO}_4$ superconductors. *Phys. Rev. Lett.* **92**, 187001 (2004).
26. Christianson, A. D. *et al.* Resonant spin excitation in the high temperature superconductor $\text{Ba}_{0.6}\text{K}_{0.4}\text{Fe}_2\text{As}_2$. *Nature* **456**, 930 (2008).
27. Richard, P. *et al.* Angle-resolved photoemission spectroscopy of the Fe-based $\text{Ba}_{0.6}\text{K}_{0.4}\text{Fe}_2\text{As}_2$ high temperature superconductor: evidence for an orbital selective electron-mode coupling. *Phys. Rev. Lett.* **102**, 047003 (2009).
28. Mazin, I. I., Singh, D. J., Johannes, M. D. & Du, M. H. Unconventional superconductivity with a sign reversal in the order parameter of $\text{LaFeAsO}_{1-x}\text{F}_x$. *Phys. Rev. Lett.* **101**, 057003 (2008).
29. Kuroki, K. *et al.* Unconventional pairing originating from the disconnected Fermi surfaces of superconducting $\text{LaFeAsO}_{1-x}\text{F}_x$. *Phys. Rev. Lett.* **101**, 087004 (2008).
30. Wang, F., Zhai, H., Ran, Y., Vishwanath, A. & Lee, D.-H. Functional renormalization-group study of the pairing symmetry and pairing mechanism of the FeAs-based high-temperature superconductor. *Phys. Rev. Lett.* **102**, 047005 (2009).
31. Seo, K., Bernevig, B. A. & Hu, J.-P. Pairing symmetry in a two-orbital exchange coupling model of oxypnictides. *Phys. Rev. Lett.* **101**, 206404 (2008).
32. Wang, F., Zhai, H. & Lee, D.-H. Antiferromagnetic correlation and the pairing mechanism of the cuprates and iron pnictides: a view from the functional renormalization group studies. *Europhys. Lett.* **85**, 37005 (2009).
33. Johannes, M. D. & Mazin, I. I. Microscopic origin of magnetism and magnetic interactions in ferropnictides. *Phys. Rev. B.* **79**, 220510(R) (2009).

Acknowledgements

We thank J.H. Bowen for proofreading our manuscript. We acknowledge the support through grants from the Chinese Academy of Sciences, NSF, Ministry of Science and Technology of China, TRIP-JST, CREST-JST, JSPS and MEXT of Japan, and NSF, DOE of US. This work was based on research conducted at the Synchrotron Radiation Center supported by NSF No. DMR-0537588.

Author contributions

Y.-M.X., P.R., K.N., T.K., Y.S., T.Q., M.N., S.S., and T.S. performed experiments. Y.-M.X., P.R. and K.N. analysed data. H.D. and Y.-M.X. designed experiments. H.D., Y.-M.X., P.R., T.S., T.T., Z.W., Z.F. and X.D. wrote the paper. H.-Q.L., H.-H.W., G.-F.C. and N.-L.W. synthesized materials. All authors discussed the results and commented on the manuscript.

Additional information

Supplementary Information accompanies this paper at <http://www.nature.com/naturecommunications>

Competing financial interests: The authors declare no competing financial interests.

Reprints and permission information is available online at <http://npg.nature.com/reprintsandpermissions/>

How to cite this article: Xu, Y.-M. *et al.* Fermi surface dichotomy of the superconducting gap and pseudogap in underdoped pnictides. *Nat. Commun.* **2**:392 doi: 10.1038/ncomms1394 (2011).